This is the accepted version of the following article:

Sun, L., Ji, X., Zhuang, Y. et al. Nonlinear modeling of the ten-story RC building structure of 2015 E-Defense shaking table tests. Bull Earthquake Eng (2023). https://doi.org/10.1007/s10518-022-01611-9.

which has been published in final form at [Link to final article]

Please cite this article as: Sun, L., Ji, X., Zhuang, Y. et al. Nonlinear modeling of the ten-story RC building structure of 2015 E-Defense shaking table tests. Bull Earthquake Eng (2023). https://doi.org/10.1007/s10518-022-01611-9.

Nonlinear modeling of the ten-story RC building structure of 2015 E-Defense shaking table tests

Lei Sun[1], Xiaodong Ji[1], Yuncheng Zhuang[1], Koichi Kajiwara[2], Jae-Do Kang[2,3], Takuya Nagae[2,4]

1. Key Laboratory of Civil Engineering Safety and Durability of China Education Ministry, Tsinghua University, Beijing, China

2. Earthquake Disaster Mitigation Research Division, National Research Institute for Earth Science and Disaster Resilience, Miki, Japan

3. Earthquake Disaster Mitigation Center, Seoul Institute of Technology, Seoul, Republic of Korea

4. Disaster Mitigation Research Center, Nagoya University, Nagoya, Japan

Abstract

In 2015, a full-scale ten-story reinforced concrete (RC) building structure was tested on the E-Defense shake table, the recorded test data from which provided a unique benchmark case to validate a state-of-the-art modeling approach. This paper presents the development and validation of a finite element model of the test building structure established on the OpenSees platform. In this model, RC beams and columns were simulated using the fiber-based beam-column element, and shear walls were modeled with the multi-layer shell element. The numerical model provided a reasonable estimate of the observed global responses of the test structure, including peak inter-story drifts and floor accelerations, for the wall direction. The multi-layer shell element effectively tracked the local strain, flexural and shear deformations of RC walls. Although the numerical model reasonably captured responses for the frame direction under base fixed JMA-Kobe 50% shaking, the simulation of RC frames was less accurate for base fixed JMA-Kobe 100% shaking when the test structure experienced significant damage at the maximum inter-story drift of 2.9%. Finally, a couple of important modeling issues for RC structure were discussed, including beam-column joint modeling and damping modeling. Use of the scissors model to represent the beam-column joints led to an improved estimation of the inter-story drifts of stories where the beam-to-column joints experienced severe damage. A transient Rayleigh damping model, in which a tangent stiffness matrix was used to formulate a system damping matrix, was recommended for structural nonlinear response history analysis.

Keywords: reinforced concrete (RC) structure; E-Defense shaking table test; nonlinear response history analysis; RC wall modeling; beam-column joint modeling.

1 Introduction

Tall buildings are widely constructed in modern cities around the world. Currently, the performance-based design has been merged as an alternative to the traditional prescriptive strength-based design for tall buildings (Moehle 2008). In the performance-based seismic design framework, nonlinear response history analysis of the structural model subjected to a suite of ground motions is commonly adopted to predict building responses at varying levels of seismic intensity. Afterwards, the estimated seismic responses are compared with the acceptance criteria defined as per the target performance levels. Therefore, accurate and reliable numerical models are crucial in the implementation of the performance-based design and assessment.

In past decades, significant efforts have been made in development of numerical modeling approaches of reinforced concrete (RC) building structures. Beam-column element with hinges (Powell and Chen 1986) and fiber beam-column element (Spacone et al. 1996) are two commonly-used modeling approaches for RC beams or columns. In the former approach, the concentrated hinges are required to be defined by the phenomenological description of the overall force-deformation relationship of the component, while the latter approach calculates the force-displacement response of the component by implicit integration of flexural stresses and strains through the cross section and along the member with predefined stress-strain relationships of materials. Various conceptually different models have been developed to model

RC shear walls, such as the Multiple-Vertical-Line-Element-Model (MVLEM) (Orakcal et al. 2004, Kolozvari et al. 2021a), Shear-Flexure-Interaction Multiple-Vertical-Line-Element-Model (SFI-MVLEM) (Kolozvari et al. 2015, 2021b), multi-layer shell element model (Lu et al. 2015a), and beam-truss model (Lu and Panagiotou 2014). Due to a high level of numerical stability, the MVLEM and multi-layer shell element models are often used in structural nonlinear analysis. Scissors model (Alath and Kunnath 1995) has been developed to represent the RC beam-to-column joints, and it is often adopted in nonlinear response history analysis of building structures due to its computational efficiency. PEER/ATC 72-1 presents a compilation of the numerical modeling approaches of the structural components and systems (PEER/ATC 2010).

Currently available research which is used as a basis to justify the modeling approaches of RC structures is almost exclusively based on experimental tests of individual structural components and relative small-scale substructures. As large-scale shaking table tests on RC building structure systems are very limited except for a few (e.g., full-scale four-story structure tests in E-Defense (Gavridou et al. 2017), seven-story RC wall structure tests in UCSD (Moaveni et al. 2011)), the modeling approaches have not been well validated against the structural system-level test data. It is a clear need to conduct large-scale dynamic tests of RC tall building structures, and validate state-of-the-art modeling approaches using the experimental data.

In 2015, E-Defense conducted shaking table tests of a full-scale ten-story reinforced concrete (RC) structure, which was heavily instrumented to record the global and local responses of the test structure under various levels of seismic shaking (Kajiwara et al. 2021). The objective of this study is to validate state-of-the-art numerical models using the valuable test as a unique benchmark case, which would provide us an insight on how accurate current modeling approach is in simulating the nonlinear response responses of RC building structures. The next section presents an overview of E-Defense shaking table tests in 2015. In the third section, the modeling approach of the test structure is described in detail. The simulation results are presented in the fourth section. Finally, a couple of important modeling issues, i.e., beam-column joint modeling and damping modeling, are discussed in the fifth section.

2 Overview of E-Defense shaking table tests

2.1 Test structure and loading protocol

To obtain realistic seismic responses of high-rise buildings with sliding bases or with fixed bases, a full-scale ten-story reinforced concrete (RC) building was tested on the E-Defense shake table in 2015 using three-directional seismic motion inputs (Fig. 1) (Kajiwara et al. 2021). The test specimen had a plan dimension of 13.5 m × 9.5 m, and the total height of the ten stories was 25.75 m. The test structure comprised RC frames in the longitudinal direction (hereinafter referred to as the frame direction), and adopted the frame-wall interacting system in the transverse direction (hereinafter referred to as the wall direction) where the RC shear walls were assigned from the 1st to 7th stories.

Two sets of experiments were conducted on the test structure. First, the structure was able to move sideways with a base sliding mechanism. Cast-iron plates were placed at the bottom of the foundation base to generate a low friction coefficient (0.2-0.25) (Enokida et al. 2013). Seismic motions including 10%, 25%, 50%, and 100% JMA-Kobe were applied to the specimen in sequence during the base sliding tests. Next, the foundation beam was fixed on the shaking table and base fixed tests were conducted. The specimen was subjected to 10%, 25%, 50%, 100%, and 60% JMA-Kobe in sequence. Before and after each seismic motion shaking, a white-noise excitation was performed for system identification. The heavily instrumented test structure provided comprehensive data on structural responses, including both global responses (e.g., inter-story drifts, floor accelerations, etc.) and local responses (e.g., beam/column end rotations, deformations of beam-column joints, vertical strains of RC walls, etc.). Further details on the specimen design and test results can be found in Kajiwara et al. (2021).

Fig. 1 Photograph of the test structure

2.2 Measurement of inter-story drifts

In the shaking table tests, displacement transducers were installed in each story as illustrated in Fig. 2a. Inter-story drift was obtained by the average value of measured displacements from the upper and lower displacement transducers (d_{i1} and d_{i2} in Fig. 2a) on a supporting column, corresponding to Δ_{i2} (as illustrated in Fig. 2a). However, lateral drifts resulting from floor slab rotations (Δ_{i1} and Δ_{i3} in Fig. 2a) were not included in the measurement, which might have led to an underestimation of inter-story drifts. Double-integration of floor acceleration data is another approach for the measurement of drifts. The floor acceleration measured using accelerometers was firstly band-pass filtered (0.2-30Hz in this study) to exclude the effect of noise, and then integrated to obtain the floor velocity. Baseline correction was implemented before integrating the velocity to obtain the absolute displacement of each floor. Inter-story drift of each story was calculated from the displacement responses of the adjacent floors. Fig. 2b presents the inter-story drift ratios obtained from the two sets of measurements under 100% JMA-Kobe shaking in base fixed tests. This indicates that the two methods provided nearly identical results in the frame direction except for the fifth-story drift, while the displacement transducer measurement provided smaller results than the accelerometer measurement due to the non-negligible floor slab rotation in the wall direction. This observation is consistent with that in another shaking table test (Ji et al. 2022), in which the effect of floor slab rotation on the inter-story drift measurement was quantified. This discrepancy became more notable at upper stories because the lateral deformation in the wall direction was characterized by a flexure type mode and the floor rotation gradually increased along the increasing height of floors. Therefore, the inter-story drifts obtained by double-integration of acceleration were adopted in the following validation of the numerical simulation.

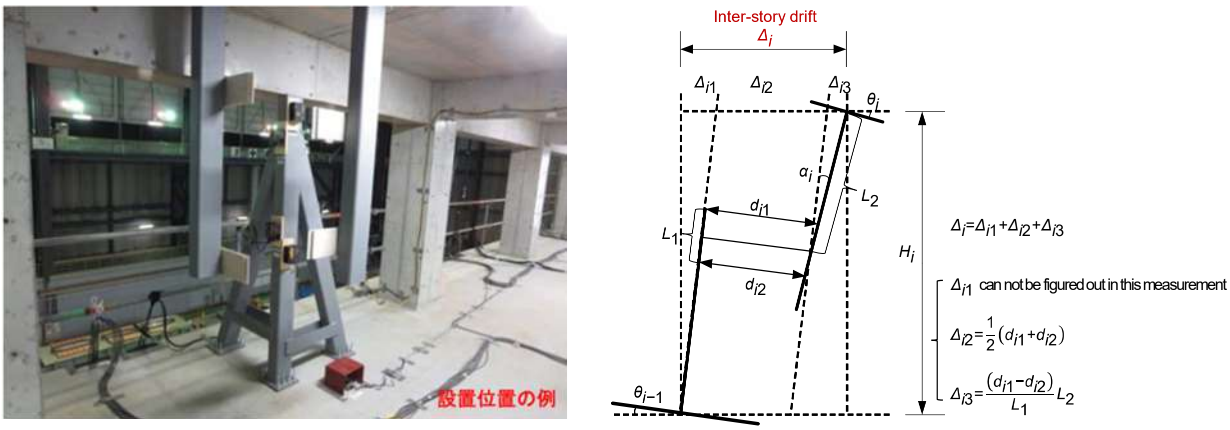

(a) Displacement transducer arrangement (b) Decomposition of measured inter-story drifts

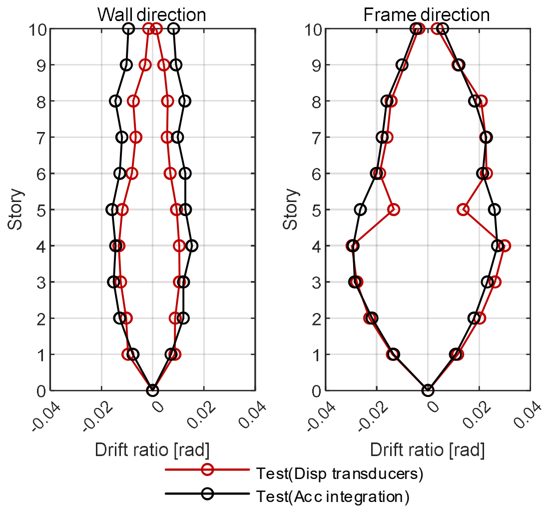

(c) Comparison between two measurements

Fig. 2 Measurements of inter-story drifts

2.3 System identification

Dynamic properties of the test structure before and after each level of seismic motion shaking were identified using the autoregressive with exogenous terms (ARX) method (Ji et al. 2011) from white noise test data. Fig. 3a depicts the identified natural vibration frequencies, damping ratios and mode shapes of the first three modes in the wall and frame directions of the undamaged test structure. Fig. 3b indicates that the first three translational modal frequencies decreased gradually after increasing levels of seismic motion shakings. After all seismic loads, the 1st modal frequency decreased by 54% in the wall direction and 77% in the frame direction, indicating severe damage and stiffness degradation of the test structure.

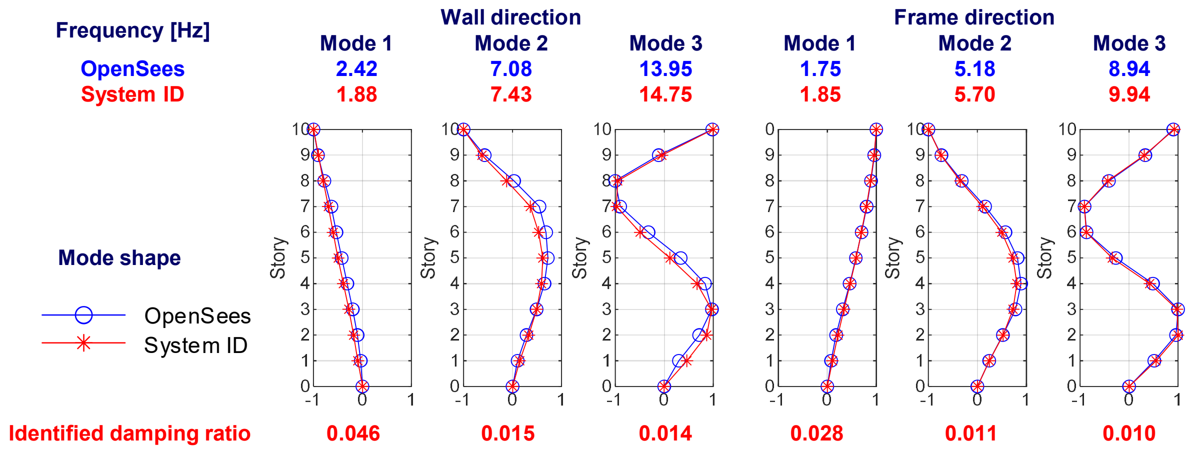

(a) Dynamic properties of the undamaged test structure

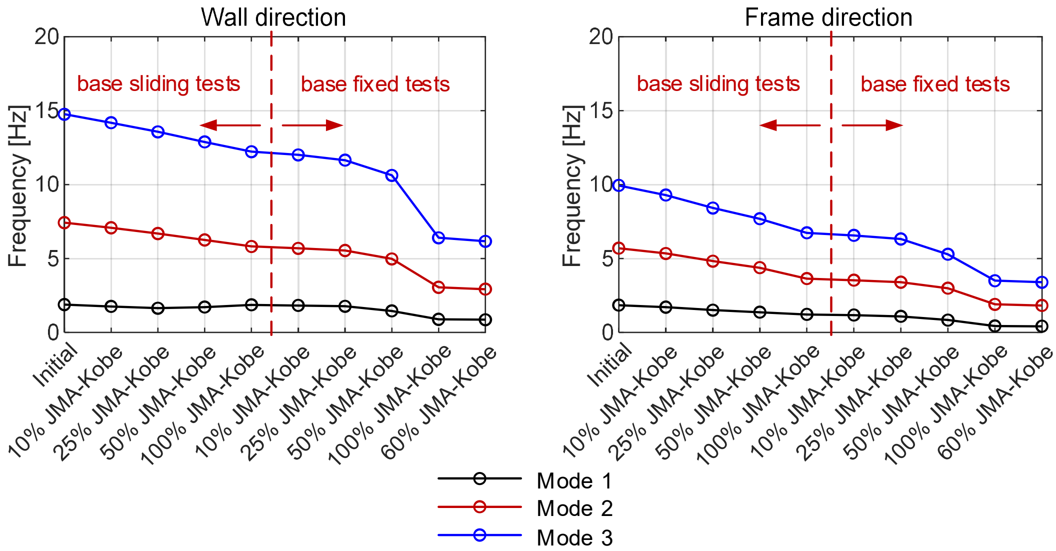

(b) Identified modal frequencies after each shaking

Fig. 3 System identification results

3 Numerical modeling approach

A numerical model was established in the structural analysis platform OpenSees (McKenna et al. 2000) according to the measured material properties and geometrical dimensions of the shaking table test structure. This section describes the details of the numerical model of the test structure.

3.1 Material modeling

The Kent-Park model (Kent and Park 1971) was adopted to define the compressive uniaxial stress-strain curve of unconfined concrete, which consists of a parabolic ascending branch and a linear descending branch. The peak stress $f_c^{'}$ was obtained from concrete cylinder tests, and the peak strain ε_{c0} was assumed to be 0.002. Elastic modulus E_{c0} was defined as $2f_c^{'}/\varepsilon_{c0}$ in this model. The stirrup-confined concrete was represented by the Saatcioglu-Razvi model (Saatcioglu and Razvi 1992), which takes into account the increase of strength and ductility caused by confining effect. The residual compressive strength was taken as zero for unconfined concrete and 0.2 times the peak strength for stirrup-confined concrete. A bilinear stress-strain curve was used to define the envelope of concrete uniaxial tensile behavior. The linear ascending branch had a slope equal to the elastic modulus of concrete in compression, and the concrete tensile strength corresponding to cracking was taken as f_t=$0.31\sqrt{f_c^{'}}$ (unit in MPa), as suggested by Berlabi and Hsu (1994). The post-cracking linear descending branch represented the tension stiffening effect of concrete, with a negative slope of 0.05 times the concrete elastic modulus. It is important to note that the hysteretic behavior of concrete in RC beams and columns followed the criteria proposed by Yassin 1994 (implemented as *Concrete02* material in OpenSees), while the concrete in RC walls was modeled with the hysteretic rules of *PlaneStressUserMaterial* (an origin-oriented linear curve was adopted for the unloading and reloading path), as illustrated in Fig. 4a. For *PlaneStressUserMaterial*, concrete was assumed to behave in a plane-stress manner, and the cracking of concrete was modeled by the fixed smeared crack approach. When the principal tensile stress exceeded the specified concrete tensile strength, cracks were assumed to occur, and concrete was treated as an orthotropic material after cracking. The reduced shear stiffness for post-cracking concrete was taken to be ηG, where G was the concrete elastic shear modulus and η was the shear retention factor to account for the post-cracking shear stiffness deterioration. The value of shear retention factor η was recommended to be approximately 0.1 (Ile and Reynouard 2000, Ji et al. 2015). In this simulation, a value of 0.08 was used for η, as determined by trial and error.

As shown in Fig. 4b, the uniaxial behavior of reinforcement was represented by the Giuffré-Menegotto-Pinto model with isotropic strain hardening (Filippou et al. 1983), which was implemented as *Steel02* material in OpenSees. This model has been well-calibrated and is capable of capturing the nonlinear hysteretic responses of reinforcement. Yield strength and elastic modulus of the reinforcement were determined by tensile tests of steel rebars, and the strain hardening ratio was set to be 0.01. The parameters which control the transition from elastic to plastic branches, including R_0, cR_1, and cR_2, were taken as 20, 0.925, and 0.15, respectively.

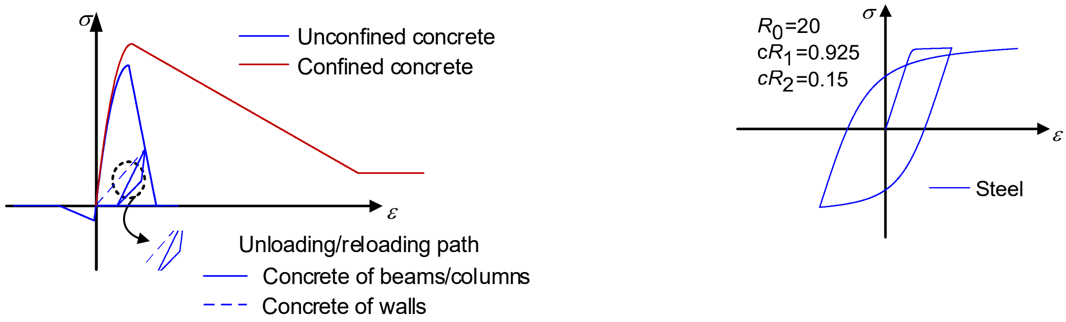

(a) Concrete (b) Steel

Fig. 4 Uniaxial stress-strain relationship of materials

3.2 Element modeling

Beams and columns in the specimen were modeled by a displacement-based beam-column element (implemented as *dispBeamColumn* in OpenSees) with a fiber section (Spacone et al. 1996), as depicted in Fig. 5a. Cover concrete, stirrup-confined concrete, and longitudinal rebars in a beam or column were represented by a number of fibers with their corresponding uniaxial constitutive relationships. Each beam or column of the test structure was discretized into five elements along the longitudinal axis with three integration points. A T-shaped cross-section was adopted for the beams to consider the slab effect. The effective overhanging flange widths of beams were determined per the Chinese design code for design of concrete structure GB50010-2010 (China Ministry of Housing and Urban-Rural Development 2015), as illustrated in Fig. 6. A rigid diaphragm was assigned to constrain all nodes at a floor level. However, this could potentially over-constrain the axial deformation of beams, resulting in unrealistic axial forces in beam elements with fiber section and overestimation of the strength capacity of the whole structure (Liu et al. 2012). To eliminate the fictitious axial forces, an "axial buffer element" (Barbagallo et al. 2020) was added in the beam end to relieve possible over-constraint on the axial deformation of beams.

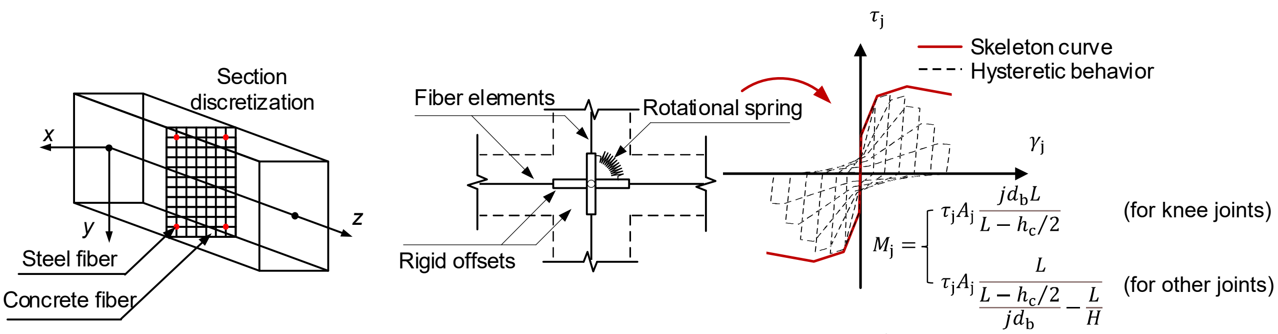

(a) RC beams and columns (b) Beam-column joints

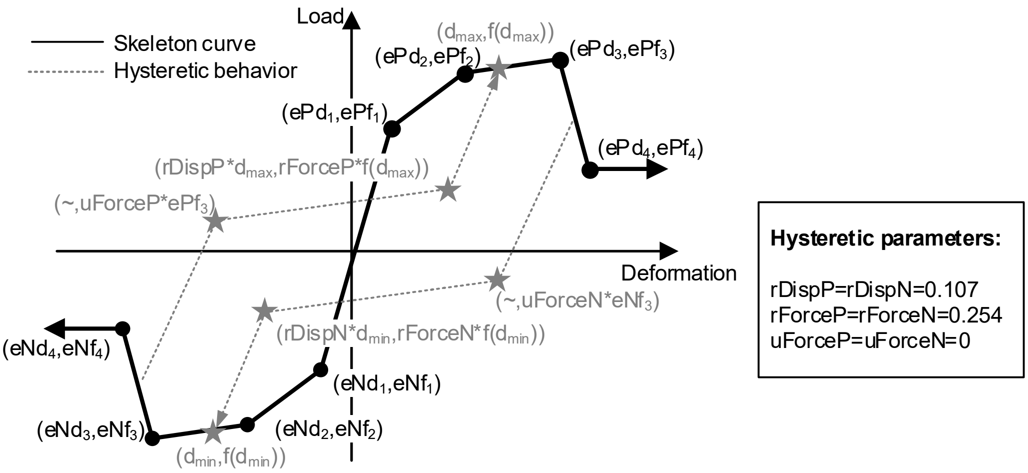

(c) Hysteretic model of beam-column joints

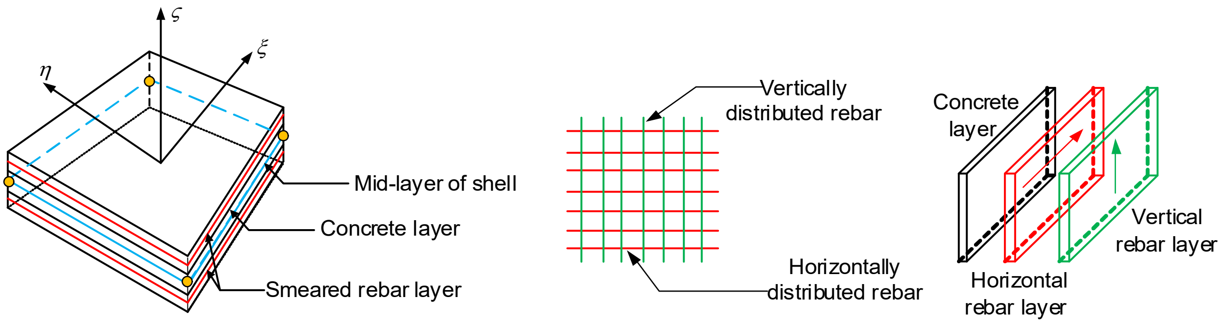

(d) RC walls

Fig. 5 Element modeling in the simulation

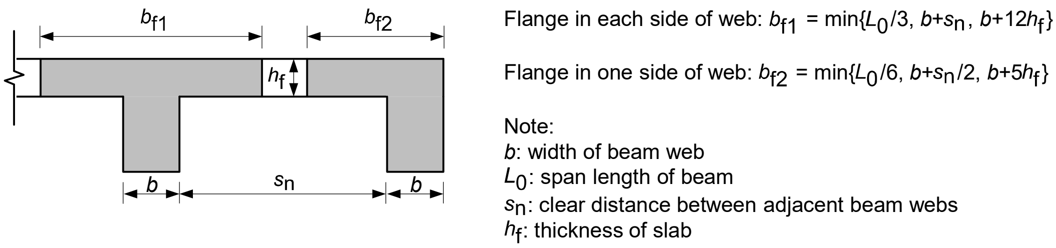

Fig. 6 Effective flange width of T-shaped beam per Chinese code GB50010-2010

Beam-column joints were represented with scissors model in both wall and frame directions, as shown in Fig. 5b. In a joint, rotational spring was represented by the *zeroLength* element, and the rigid offsets were modeled by *elasticBeamColumn* elements with rigid stiffness (using very large Young's modulus of 3e10 N/mm^2). The nonlinear joint shear stress-strain (τ_j-γ_j) relationship was modeled with the quadrilinear backbone curve proposed by Lafave and Kim (2011). The moment-rotation (M_j-θ_j) relationship was obtained using the equations in Fig. 5b (Hassan and Moehle 2012), where L is the length from the beam inflection point to the column centerline, approximated as a half beam centerline span; jd_b is the beam lever arm, which was approximated as 0.90 times the effective beam depth; H is the column height measured between column inflection points, approximated as the story height; h_c is the height of the column cross-section; and A_j is the effective joint shear area, which is taken as the product of effective joint width (average of beam and column widths) and column depth (Kim 2007). *Pinching4* material was adopted to assign the moment-rotation relationship to the joint rotational spring (*zeroLength* element). The parameters defining hysteretic responses and their values are illustrated in Fig. 5c, which have been calibrated against past test data (Theiss 2005).

RC walls in the test structure were modeled by a shell element (implemented as *ShellDKGQ* in OpenSees) with a multi-layer shell section (Lu et al. 2015), which can simulate the coupled in-plane and out-of-plane behaviors of RC walls. The multi-layer shell element for modeling structural wall components has been validated to ensure both computational efficiency and a reasonable level of accuracy (Lu et al. 2013, Ji et al. 2015). It consists of a number of concrete layers and rebar layers (Fig. 5d). Different layers in the shell element were assumed to be fully bonded in the thickness direction, and the deformation of each layer was obtained from that of the middle layer based on the plane-section assumption. For the wall webs, the cover and inside concrete were represented by a number of unconfined concrete layers, and the distributed reinforcements were represented by the smeared rebar layers in vertical and horizontal directions, respectively. For the boundary elements, the longitudinal rebars were modeled with truss elements, and the boundary core concrete was represented by stirrup-confined concrete layers. Each wall at a story was discretized into five by ten meshes in the vertical and horizontal direction, respectively, and sixteen layers in the thickness direction.

3.3 Mass, damping, loading, and boundary conditions

Tributary mass was assigned at the wall and column nodes at each floor level along with the tributary gravity load (dead and live). Rayleigh damping with a tangent stiffness matrix was adopted for structural damping modeling. Fig. 3a presents the first three translational modal damping ratios in the wall and frame directions of the test structure at the initial state, which was identified from the white noise test data. Note that in the system identification, the apparent damping induced by pitching of shaking table was removed (Molina et al. 2008). In the wall direction, the average damping ratio of the first three modes was 0.025, and that in the frame direction was 0.016. In addition, ASCE 7-16 (American Society of Civil Engineers 2016) specifies that the inherent damping of a structure shall not exceed 0.025 equivalent viscous damping in the significant modes of responses. Therefore, damping coefficients were formulated by setting a damping ratio of 0.025 for the 1st and 9th structural modes (corresponding to the 1st translational mode in the frame direction and 3rd translational mode in the wall direction, respectively). In the calculation of Rayleigh damping coefficients, modal frequencies were obtained from system identification using white noise test data and updated after each seismic motion shaking.

The foundation beams of the test structure were not modeled. All the degrees of freedom (DOF) of nodes at column bases were fully fixed, and the nodes of wall bottom were pinned at the base. The shaking table test consisted of two phases: the base sliding phase and base fixed phase. For the nonlinear response history analysis, three-directional acceleration data measured at the foundation top face of the test specimen were used as the seismic input. Therefore, the sliding behavior of the foundation was not explicitly simulated. All seismic motion inputs were applied consecutively in the numerical simulation to reflect the effect of cumulative damage to the test structure. P-Delta effects were considered in the modeling. Newmark-β method and ModifiedNewton algorithm were adopted in the nonlinear response history analysis with *NormDispIncr* for convergence test. In each loading step, the tolerance for convergence test was 0.001 m and the maximum number of iterations was 100.

4 Numerical simulation results

This section presents comparisons of experimental and analytical responses (e.g., inter-story drift, floor acceleration, base shear force, overturning moment, and local responses) particularly for base fixed 50% and 100% JMA-Kobe shaking tests, as the test structure exhibited obvious nonlinear responses in these loading cases.

4.1 Dynamic properties

Modal analysis of the numerical model estimated the natural vibration frequencies and associated mode shapes of the test structure. As shown in Fig. 3a, the dynamic properties of the initial test structure estimated by the numerical model correlated well with the system identification results, except for some discrepancy in the 1st modal frequency of the wall direction. This discrepancy was because the base sliding foundation was not explicitly simulated in the numerical model. The test structure was able to move sideways with a base sliding mechanism in the initial state and base uplifting in the wall direction was observed during the white noise test (Tosauchi et al. 2018), while those boundary conditions were not considered in the numerical model. Nevertheless, such discrepancy would not influence the nonlinear response simulation of base fixed 50% and 100% JMA-Kobe loading cases which is the highlight of the study, as in such loading cases the foundation beams were fully anchored on the shaking table.

4.2 Response envelopes

Figs. 7 and 8 depict the peak inter-story drift ratios and peak floor accelerations distributed along the height of the test structure when subjected to 50% and 100% JMA-Kobe motions (base fixed tests). As indicated in Fig. 7a, when subjected to 50% JMA-Kobe, the calculated peak drift values and their distribution along the structural height aligned well with the test data in the frame direction, while somewhat discrepancy is found in the wall direction. The average error of the numerical results relative to the test data was 17.5% and 17.0% for the peak floor acceleration in the wall and frame direction, respectively, as shown in Fig. 8a. The numerical model is able to capture global seismic responses with reasonable accuracy when the structure is in a moderate nonlinear state. Under 100% JMA-Kobe motion, the numerical model was still able to provide a reasonable estimate of the inter-story drifts and floor accelerations of the structure in the wall direction (see Fig. 7b and Fig. 8b). However, the discrepancy between the numerical simulation and test data became notable for the frame direction, with the average errors of the peak inter-story drifts and floor accelerations for all floors increasing to 41.1% and 34.4%, respectively. The increased errors in severe nonlinear states (the maximum inter-story drift ratio reaching 2.9%) might be due to the modeling of floor slab contribution. In this model, slab contribution was considered by T-shaped cross-section beams, and the effective overhanging flange width of each beam was taken as a fixed value per the Chinese design code for design of concrete structure GB 50010-2010 (China Ministry of Housing and Urban-Rural Development 2015). However, it was revealed that effective overhanging flange widths of beams would change under different inter-story drifts (Ning et al. 2014). In addition, Fig. 7b indicates that although the numerical simulation could accurately predict the maximum inter-story drift in the 4^{th} story, this resulted in an overly concentrated drift distribution and an underestimate of the inter-story drift at upper stories. This discrepancy is related to the beam-to-column joint modeling, and will be discussed in section 5.1.

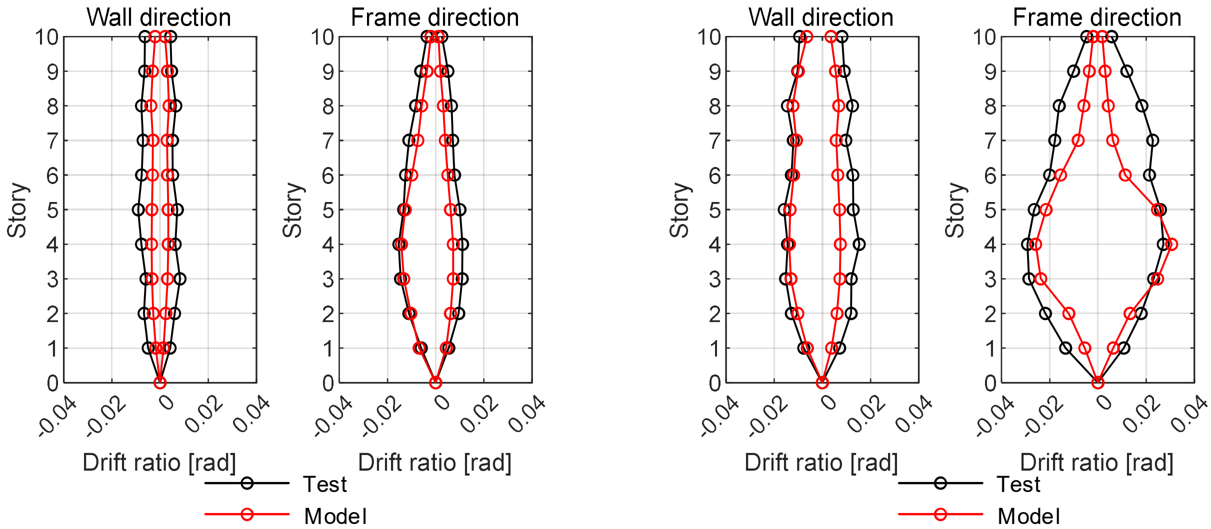

(a) Base fixed 50% JMA-Kobe (b) Base fixed 100% JMA-Kobe

Fig. 7 Inter-story drift ratios along the specimen height

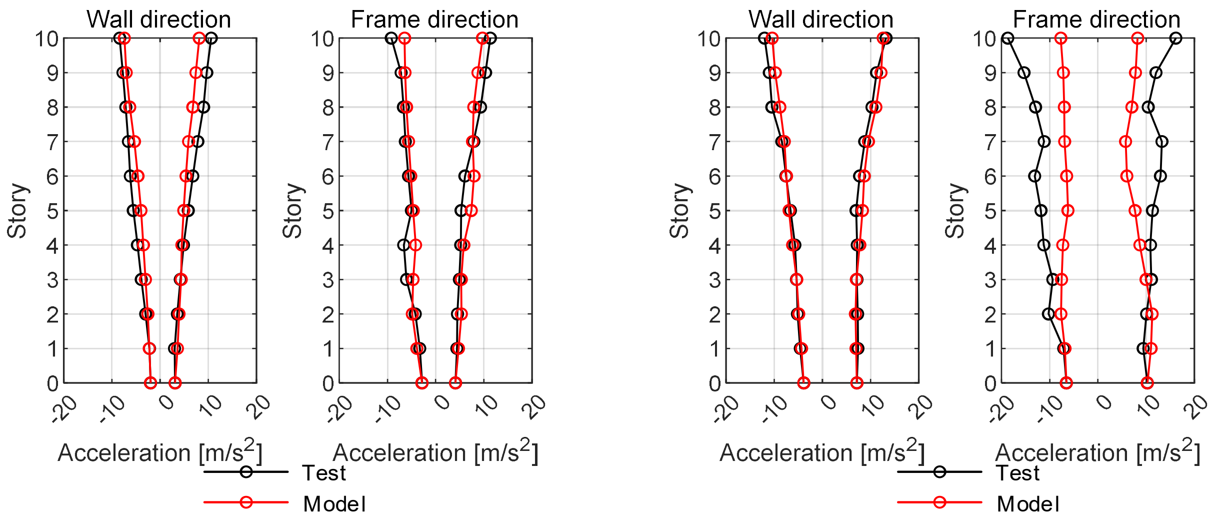

(a) Base fixed 50% JMA-Kobe (b) Base fixed 100% JMA-Kobe

Fig. 8 Floor accelerations along the specimen height

4.3 Base shear force and overturning moment

Fig. 9 compares the numerical results and test data for the base shear force and overturning moment of the test structure. It is important to note that the values were calculated from the measured/calculated floor accelerations, floor masses and floor heights. The numerical model reasonably tracked the base shear force and overturning moment responses with the test results, for both 50% and 100% JMA-Kobe loadings.

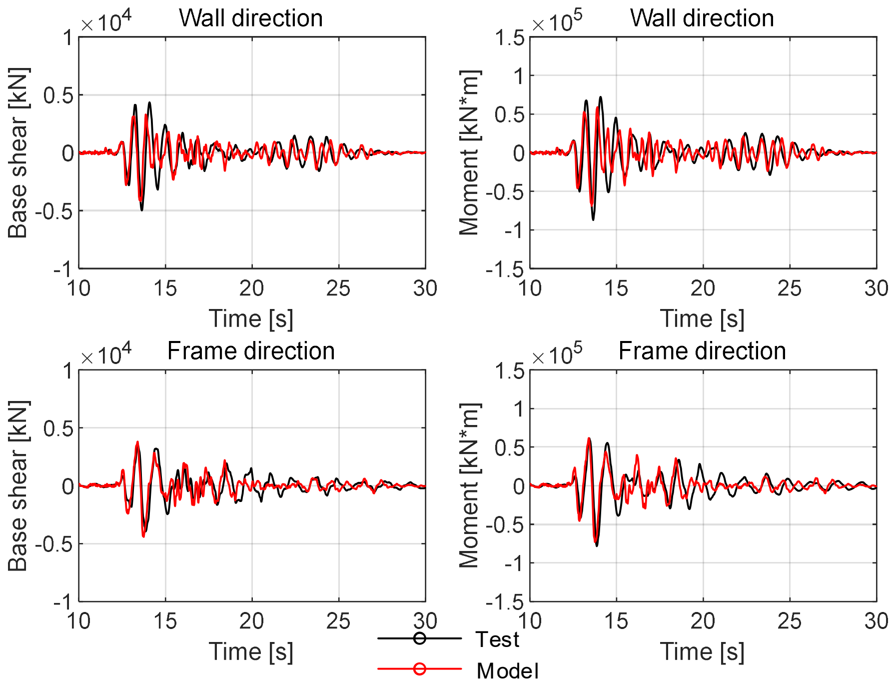

(a) Base fixed 50% JMA-Kobe

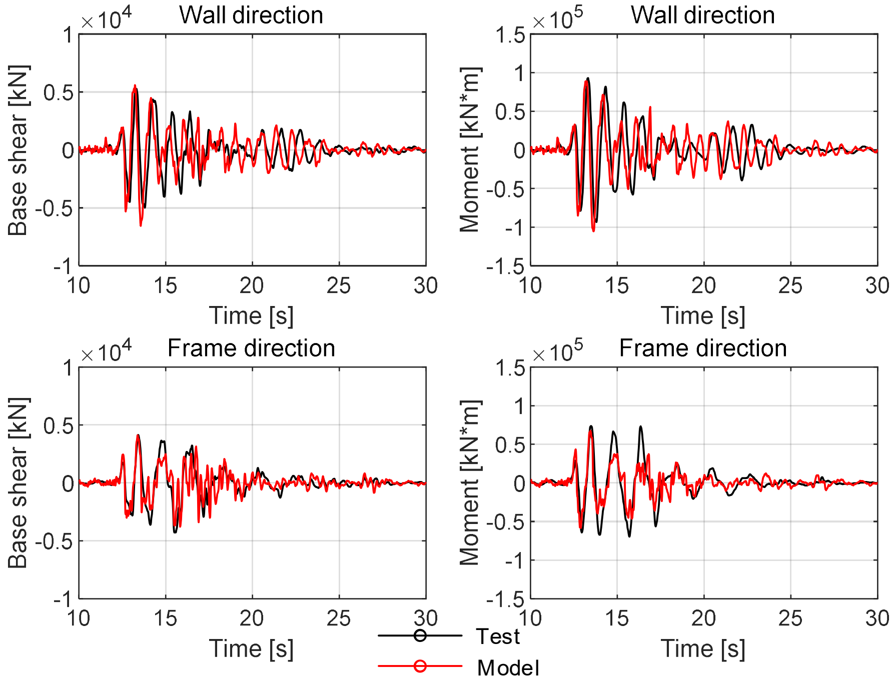

(b) Base fixed 100% JMA-Kobe

Fig. 9 Base shear force and overturning moment history responses

4.4 Local behavior of RC walls

The capability of the multi-layer shell element to capture the local behavior of RC walls in the test structure was also assessed. Using the measured data of the displacement transducers (as shown in Fig. 10), the average vertical strains along the wall edges were obtained and the flexural and shear deformation contributions were calculated (Massone and Wallace 2004). Note that local responses of RC walls were only measured on the bottom three stories. Fig. 11a demonstrates that the numerical model accurately captured the boundary vertical strains, flexural and shear deformations in the bottom three stories for 50% JMA-Kobe loading. Under 100% JMA-Kobe loading, the numerical model also reasonably captured the flexural and shear deformation of RC walls. The experimental data indicated that shear deformation contributed 28.9% to the lateral drift of the 1st-story wall, and the numerical simulation estimated 20.5% contribution of shear deformation to the drift. The wall's boundary vertical strains were estimated with good accuracy in the 1st (upper part), 2nd and 3rd stories. However, a notable discrepancy was evident in the lower part (approximately 0.2 times the wall sectional depth) the 1st-story wall, where the measured tensile strains were significantly larger than the estimated results (see Fig. 11b). This discrepancy was because the bottom vertical displacement transducers were end to the foundation beam (see Fig. 10), such that the cracks developed at the wall-foundation beam interface would lead to the increase of measured average tensile strain. However, the numerical model did not simulate the wall-foundation beam interface behavior.

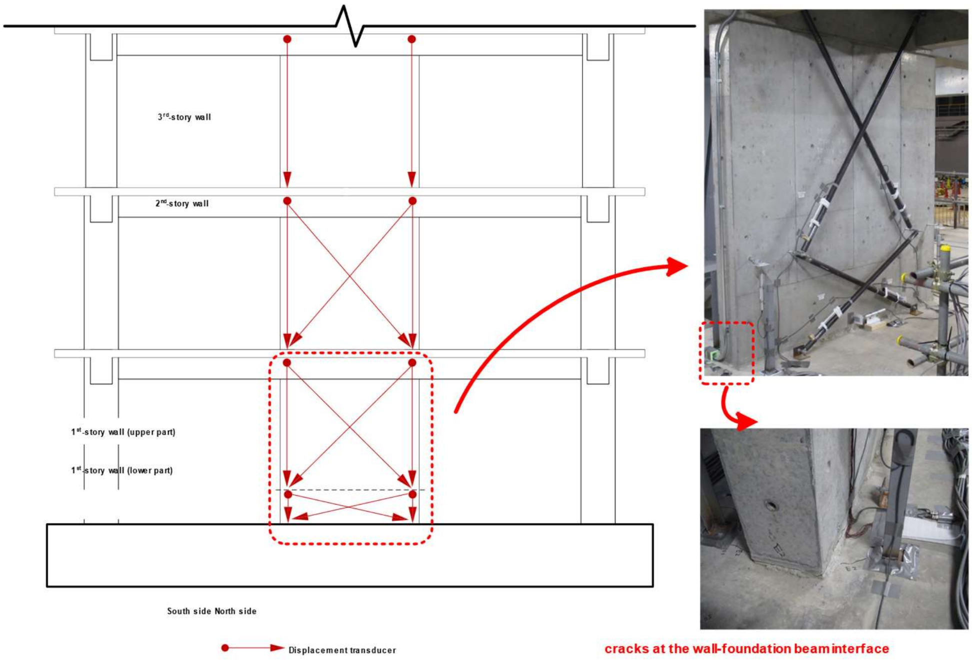

Fig. 10 Displacement transducers on RC walls

Vertical strains (at the north side of walls) | Response envelopes | Vertical strains (at the north side of walls) | Response envelopes

Test
Model

Test
Model

(a) Base fixed 50% JMA-Kobe (b) Base fixed 100% JMA-Kobe

Fig. 11 Local responses of RC walls

5 Discussions of modeling issues

5.1 Beam-column joint modeling

Due to insufficient transverse reinforcement, the beam-column joints of the test structure underwent severe damage during the tests. The video records revealed diagonal cracks and slight concrete spalling when subjected to 100% JMA-Kobe in base fixed tests (Fig. 12). The scissors model was adopted to incorporate beam-column joints into the numerical model, as presented in section 3 (referred to as Model-W-joint in this section). To investigate the effect of beam-column joint modeling on the simulation results, another model of the test structure was established for comparison, in which the beam-column joints were not modeled, and fiber beams and columns were directly connected at the intersection of their centerlines (referred to as Model-WO-joint in this section).

(a) After base fixed 50% JMA-Kobe (b) After base fixed 100% JMA-Kobe

Fig. 12 Damage states of a beam-column joint of the 5th floor

Fig. 13 compares the maximum inter-story drift ratios in the frame direction estimated by the Model-W-joint and Model-WO-joint models. This demonstrates that when subjected to 25% and 50% JMA-Kobe (base fixed), there was no obvious difference between the results from Model-W-joint and Model-WO-joint, as the beam-to-column joints did not sustain significant damage under those shakings. Under base fixed 100% JMA-Kobe, significant drifts (2.6% to 2.9% drift ratio) occurred in the 3rd to 5th stories, but were evidently underestimated by Model-WO-joint. When applying the scissors model to represent the joint nonlinear behavior, the Model-W-joint exhibited improved accuracy in simulating the large inter-story drift of the 3rd to 5th stories. The simulation error of the maximum inter-story drift ratio in the 4th story decreased from 19.6% to 4.8% when considering the beam-to-column joint model.

Test
Model-W-joint
Model-WO-joint

Test
Model-W-joint
Model-WO-joint

Test
Model-W-joint
Model-WO-joint

(a) Base fixed 25% JMA-Kobe (b) Base fixed 50% JMA-Kobe (c) Base fixed 100% JMA-Kobe

Fig. 13 Effect of joint modeling on the inter-story drift ratios from simulation

The calculated shear deformations of beam-to-column joint zones were further compared with the test data. As shown in Fig. 14, shear deformations of the joints on the 2nd to 5th and 7th floors were measured by inclined LVDTs. Fig. 15 indicates that the Model-W-joint effectively captured the joint deformations under 25% and 50% JMA-Kobe. When subjected to 100% JMA-Kobe, significant joint deformations developed. Although the joint model provided an accurate estimate of the shear deformation of the joints of the 2nd and 3rd floors (i.e., JNT1 and JNT2 in Fig. 14), it overestimated the deformation of the joints of the 4th and 5th floors (i.e., JNT3 and JNT4) and underestimated the deformation of the joint of the 7th floor (i.e., JNT6). This discrepancy local joint deformation is consistent with the estimated results of the global inter-story drift presented in Fig. 13c. The errors are suspicious to be related to the determination of parameter values of the scissors model, thus indicating a need for improvement of the scissors model in future.

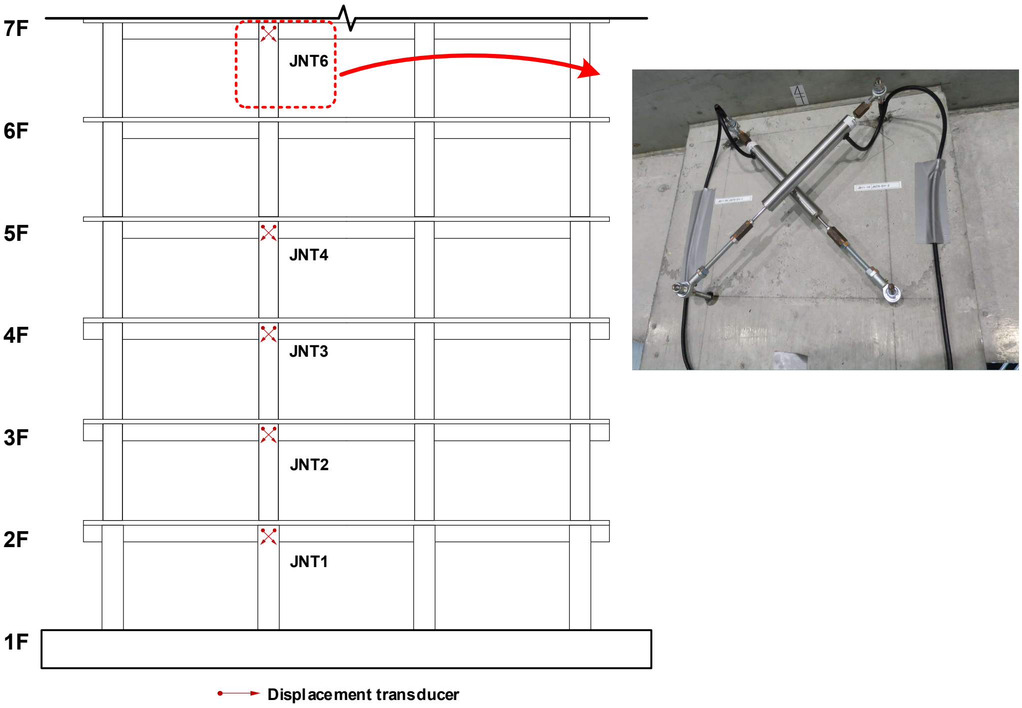

Fig. 14 Measurement of joint deformations

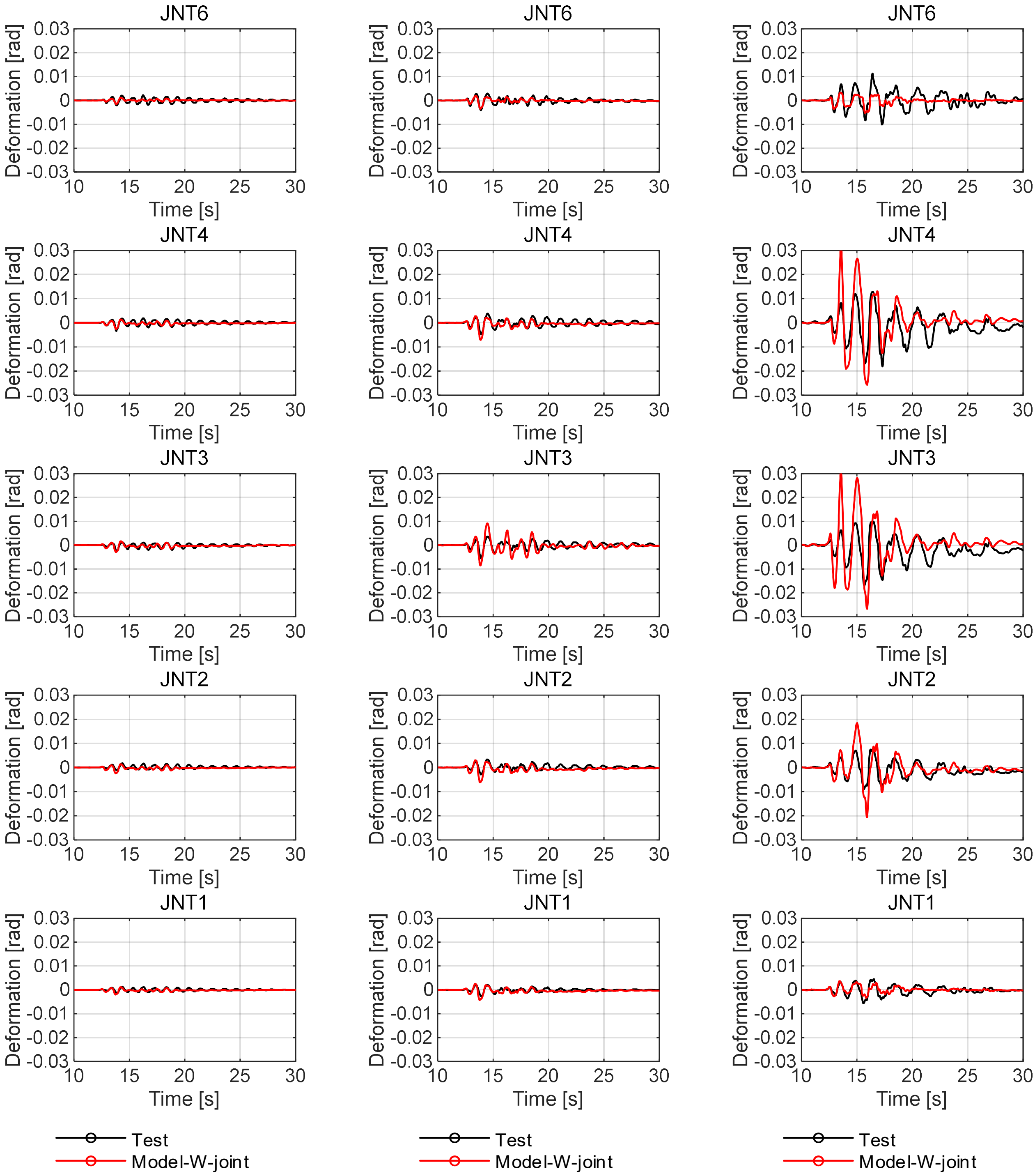

(a) Base fixed 25% JMA-Kobe (b) Base fixed 50% JMA-Kobe (c) Base fixed 100% JMA-Kobe

Fig. 15 Joint deformations from experimental and numerical results

5.2 Damping modeling

Classical damping (such as Rayleigh damping) is appropriate if similar damping mechanisms are distributed throughout the structure, and the Rayleigh damping model has been widely adopted in structural nonlinear analysis due to its simplicity. However, structural damping may be significantly amplified to an unrealistic state when Rayleigh damping is formulated by the structural initial stiffness matrix (Charney 2008, Jehel et al. 2014). Therefore, a "transient" Rayleigh damping model was adopted (as illustrated in section 3.3, referred to as Model-T-damping in this section) for the simulation.

To quantify the effect of damping modeling on the structural responses from simulation, another structural model with "initial" Rayleigh damping was established (referred to as Model-I-damping in this section), where the initial stiffness matrix was utilized to construct the Rayleigh damping. Rayleigh proportionality coefficients were determined by modal damping ratios and modal frequencies. In both models, a damping ratio of 0.025 was set for the 1st and 9th structural mode and assumed to be constant during the tests, and the modal frequencies for damping formulation were updated after each shaking by system identification, which also updated the Rayleigh proportionality coefficients.

Fig. 16 compares the inter-story drifts from the Model-T-damping and Model-I-damping against test data. Under base fixed 50% JMA-Kobe shaking, both models had similar estimation of the inter-story drifts. However, a notable difference was observed for the fixed 100% JMA-Kobe loading case, when the structure underwent significant nonlinearity. Particularly for the wall direction, a notable improvement in simulation accuracy for the model using "transient" Rayleigh damping can be observed, relative to "initial" Rayleigh damping. Therefore, the modeling approach of Rayleigh damping has a non-negligible influence on the structural responses, and transient Rayleigh damping is recommended for use in numerical modeling.

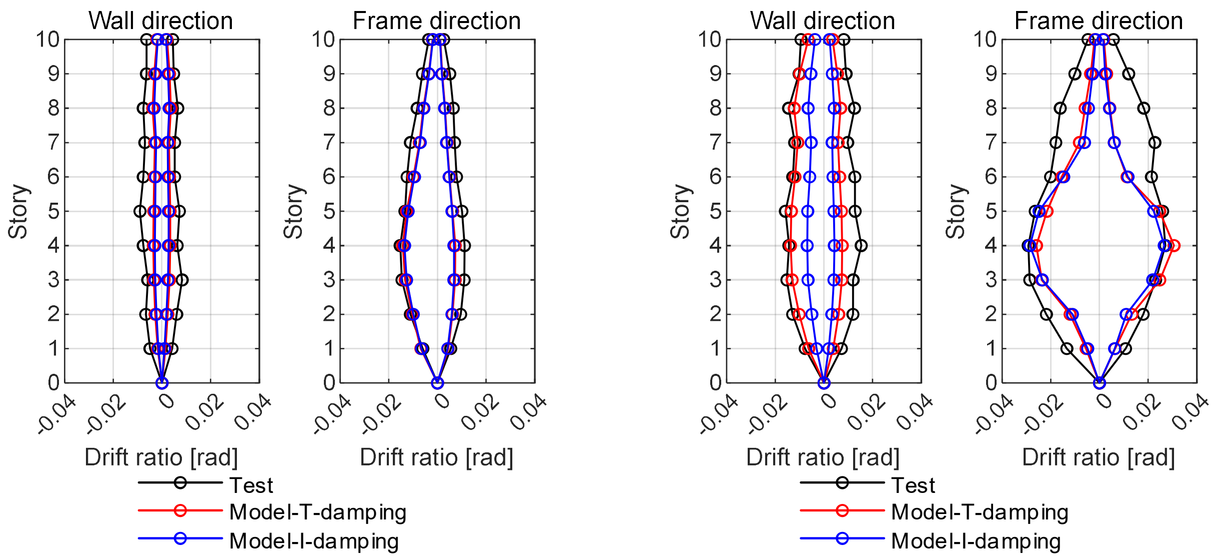

(a) Base fixed 50% JMA-Kobe (b) Base fixed 100% JMA-Kobe

Fig. 16 Effect of damping modeling on the inter-story drift ratios from simulation

6 Conclusions

Shaking table tests of a full-scale ten-story RC building structure conducted at E-Defense provided a unique benchmark case for validation of state-of-the-art numerical modeling of RC structures. In this study, a numerical model of the test structure was established in OpenSees, which adopted a fiber-based beam-column element for RC beams/columns, multi-layer shell element for RC walls, and scissors model for beam-to-column joints. The simulation results were compared against test data to assess the ability of the numerical model to capture the structural nonlinear dynamic responses. Based on the results, the following conclusions can be drawn.

(1) The numerical model provided reasonable simulations of observed global responses, including peak inter-story drift ratios, floor accelerations, base shear forces and overturning moments of the test structure within a moderate nonlinear state (e.g., under 50% JMA-Kobe motion). For 100% JMA-Kobe motion loading, the numerical model could also reasonably predict the peak inter-story drift in the wall direction, with an average error of 14.8%. However, a notable

discrepancy was observed between the numerical results and test data of the structural responses in the frame direction, indicating the numerical model is less accurate for the simulation of significant seismic damage and severe nonlinear response (peak inter-story drift reaching 2.9%).

(2) The multi-layer shell element model reasonably predicted the flexural and shear deformations of RC walls in the bottom three stories. The average boundary vertical strains of RC walls estimated by the numerical model also matched well with the measured test data, except for a discrepancy at the wall's bottom vertical tensile strain because the measured data was influenced by the wall-foundation beam interface cracks.

(3) When subjected to 100% JMA-Kobe, the beam-to-column joints of the 4th to 6th floors were significantly damaged. The numerical model without beam-column joint modeling underestimated the inter-story drift ratios of the 3rd to 5th stories. By incorporating the scissors model to represent the nonlinear behavior of the beam-column joints, the numerical model provided an improved estimate of the inter-story drifts of stories where the beam-to-column joints experienced severe damage. Nevertheless, the calculated shear deformations of beam-to-column joint zones had non-negligible discrepancy with the experimental test data, indicating the necessity for further improvement of beam-to-column joint modeling.

(4) The modeling approach of Rayleigh damping has a non-negligible influence on the structural nonlinear responses. A tangent stiffness matrix is recommended to formulate a system damping matrix, and Rayleigh proportionality coefficients should be updated after each seismic loading to reflect the effect of a decrease in frequency.

Acknowledgements

The authors appreciate the National Research Institute for Earth Science and Disaster Resilience (NIED) for providing the E-Defense shaking table test data of the 10-story RC building structure. The first three authors are sponsored by the fund from the National Natural Science Foundation of China (Grant No. 52078277), and they are sincerely grateful to the sponsor.

References

Alath S, Kunnath S (1995) Modeling inelastic shear deformation in RC beam-column joints. Proc the 10th Conf Eng Mech, University of Colorado at Boulder, Boulder, Colorado.

American Society of Civil Engineers (2016) Minimum design loads for buildings and other Structures. ASCE/SEI 7-16, Reston, VA: ASCE. https://doi.org/10.1061/9780784414248

Barbagallo F, Bosco M, Marino EM, Rossi PP (2020) On the fibre modelling of beams in RC framed buildings with rigid diaphragm. Bull Earthq Eng 18:189–210. https://doi.org/10.1007/s10518-019-00723-z

Belarbi A, Hsu TTC (1994) Constitutive laws of concrete in tension and reinforcing bars stiffened by concrete. ACI Struct J 91:465–474. https://doi.org/10.14359/4154

Charney FA (2008) Unintended consequences of modeling damping in structures. J Struct Eng 134:581–592. https://doi.org/10.1061/(ASCE)0733-9445(2008)134:4(581)

China Ministry of Housing and Urban-Rural Development (2015) Code for design of concrete structures (GB 50010-2010). China Architecture & Building Press, Beijing. (in Chinese)

China Ministry of Housing and Urban-Rural Development (2016) Code for seismic design of buildings (GB 50011-2010). China Architecture & Building Press, Beijing. (in Chinese)

Enokida R, Nagae T, Ikenaga M, et al. (2013) Application of graphite lubrication for column base in free standing steel structure. J Struct Constr Eng 78:435-444. https://doi.org/10.3130/aijs.78.435 (in Japanese)

Filippou FC, Popov EP, Bertero VV (1983) Effects of bond deterioration on hysteretic behavior of reinforced concrete joint (EERC 83-19). Earthquake Engineering Research Center, University of California, Berkeley

Gavridou S, Wallace JW, Nagae T, et al. (2017) Shake-table test of a full-scale 4-story precast concrete building. I:

Overview and experimental results. J Struct Eng 143(6):04017034. https://doi.org/10.1061/(ASCE)ST.1943-541X.0001755

Hassan WM, Moehle JP (2012) A cyclic nonlinear macro model for numerical simulation of beam-column joints in existing concrete buildings. Proc the15th World Conf Earthq Eng

Ile N, Reynouard JM (2000) Nonlinear analysis of reinforced concrete shear wall under earthquake loading. J Earthq Eng 4:183–213. https://doi.org/10.1080/13632460009350368

Jehel P, Léger P, Ibrahimbegovic A (2014) Initial versus tangent stiffness-based Rayleigh damping in inelastic time history seismic analyses. Earthq Eng Struct Dyn 43:467–484. https://doi.org/10.1002/eqe.2357

Ji X, Fenves GL, Kajiwara K, Nakashima M (2011) Seismic damage detection of a full-scale shaking table test structure. J Struct Eng 137:14–21. https://doi.org/10.1061/(asce)st.1943-541x.0000278

Ji X, Gao X, Zhuang Y, Qu Z (2022). Enhanced measurements of structural inter-story drift responses in shaking table tests. Eng Struct, in press.

Ji X, Sun Y, Qian J, Lu X (2015) Seismic behavior and modeling of steel reinforced concrete (SRC) walls. Earthq Eng Struct Dyn 44:955–972. https://doi.org/10.1002/eqe.2494

Kajiwara K, Tosauchi Y, Kang JD, et al. (2021) Shaking-table tests of a full-scale ten-story reinforced-concrete building (FY2015). Phase I: Free-standing system with base sliding and uplifting. Eng Struct 233:111848. https://doi.org/10.1016/j.engstruct.2020.111848

Kent DC, Park R (1971) Flexural members with confined concrete. J Struct Div 97:1969–1990. https://doi.org/10.1061/JSDEAG.0002957

Kim JH (2007) Joint shear behavior of reinforced concrete beam-column connections subjected to seismic lateral loading. Dissertation, University of Illinois at Urbana-Champaign

Kolozvari K, Orakcal K, Wallace JW (2015) Modeling of cyclic shear-flexure interaction in reinforced concrete structural walls. I: Theory. J Struct Eng 141(5):04014135. https://doi.org/10.1061/(asce)st.1943-541x.0001059

Kolozvari K, Kalbasi K, Orakcal K, Wallace J (2021a) Three-dimensional model for nonlinear analysis of slender flanged reinforced concrete walls. Eng Struct 236:112105. https://doi.org/10.1016/j.engstruct.2021.112105

Kolozvari K, Kalbasi K, Orakcal K, Wallace J (2021b) Three-dimensional shear-flexure interaction model for analysis of non-planar reinforced concrete walls. J Build Eng 44:102946. https://doi.org/10.1016/j.jobe.2021.102946

LaFave JM, Kim JH (2011) Joint shear behavior prediction for RC beam-column connections. Int J Concr Struct Mater 5:57–64. https://doi.org/10.4334/ijcsm.2011.5.1.057

Liu Y, Shiohara H, Nagae T, Matsumori T (2012) A simulation of three dimensional shaking table tests on a full-scale four-story reinforced concrete building. Proc the15th World Conf Earthq Eng

Lowes LN, Altoontash A (2003) Modeling reinforced-concrete beam-column joints subjected to cyclic loading. J Struct Eng 129:1686–1697. https://doi.org/10.1061/(asce)0733-9445(2003)129:12(1686)

Lu X, Lu X, Guan H, Ye L (2013) Collapse simulation of reinforced concrete high-rise building induced by extreme earthquakes. Earthq Eng Struct Dyn 42:705–723. https://doi.org/10.1002/eqe.2240

Lu X, Xie L, Guan H, Huang YL, Lu X (2015a) A shear wall element for nonlinear seismic analysis of super-tall buildings using OpenSees. Finite Elem Anal Des 98:14–25. https://doi.org/10.1016/j.finel.2015.01.006

Lu X, Zhou B, Zhao B, Lu W (2015b) Shaking table test and numerical analysis of a high-rise building with steel reinforce concrete column and reinforce concrete core tube. Struct Des Tall Spec Build 24:1019-1037. https://doi.org/10.1002/tal.1224

Lu Y, Panagiotou M (2014) Three-dimensional cyclic beam-truss model for nonplanar reinforced concrete walls. J Struct Eng 140(3): 04013071. https://doi.org/10.1061/(ASCE)ST.1943-541X.0000852

Massone LM, Wallace JW (2004) Load-deformation responses of slender reinforced concrete walls. ACI Struct J 101:103–113. https://doi.org/10.14359/13003

McKenna F, Fenves GL, Scott MH (2000) Open system for earthquake engineering simulation. University of California, Berkeley

Moaveni B, He X, Conte JP, et al. (2011) System identification study of a 7-story full-scale building slice tested on the UCSD-NEES shake table. J Struct Eng 137(6):705–717. http://doi.org/10.1061/(ASCE)ST.1943-541X.0000300

Moehle JP (2008) Performance-based seismic design of tall buildings in the US. Proc the14th World Conf Earthq Eng

Molina FJ, Magonette G, Viaccoz B, et al. (2008) Apparent damping induced by spurious pitching in shaking-table testing. Earthq Eng Struct Dyn 37(1):103–119. https://doi.org/10.1002/eqe.747

Ning N, Qu W, Zhu P (2014) Role of cast-in situ slabs in RC frames under low frequency cyclic load. Eng Struct 59:28–38. https://doi.org/10.1016/j.engstruct.2013.09.050

Orakcal K, Wallace JW Conte JP (2004) Flexural modeling of reinforced concrete walls–model attributes. ACI Struct J 101(5):688–698. https://doi.org/10.14359/13391

PEER/ATC (2010) Modeling and acceptance criteria for seismic design and analysis of tall buildings, PEER/ATC 72–1. Prepared for Pacific Earthquake Engineering Research Center (PEER) by Applied Technology Council (ATC), Redwood City, San Diego

Powell GH, Chen PF (1986) 3D beam-column element with generalized plastic hinges. J Eng Mech 112:627–641. https://doi.org/10.1061/(asce)0733-9399(1986)112:7(627)

Rots JG, Blaauwendraad J (1989) Crack models for concrete: discrete or smeared? Fixed multi-directional or rotatin? HERON 34:3–59

Saatcioglu M, Razvi SR (1992) Strength and ductility of confined concrete. J Struct Eng 118:1590–1607. https://doi.org/10.1061/(asce)0733-9445(1992)118:6(1590)

Spacone E, Filippou FC, Taucer FF (1996) Fibre beam-column model for non-linear analysis of R/C frames: Part I. Formulation. Earthq Eng Struct Dyn 25:711–725. https://doi.org/10.1002/(SICI)1096-9845(199607)25:7<711::AID-EQE576>3.0.CO;2-9

Telleen K, Maffei J, Heintz J, Dragovich J (2012) Practical lessons for concrete wall design, based on studies of the 2010 Chile earthquake. Proc the15th World Conf Earthq Eng

Theiss AG (2005) Modeling the earthquake response of older reinforced concrete beam-column building joints. Dissertation, University of Washington

Tosauchi Y, Sato E, Fukuyama K, et al. (2018) Three-dimensional shaking table test of a ten story RC frame (2015): test methods and the responses in case of sliding bases. J Struct Constr Eng 83(750): 1139–1149. https://doi.org/10.3130/aijs.83.1139 (in Japanese)

Yassin MHM (1994) Nonlinear analysis of prestressed concrete structures under monotonic and cyclic loads. Dissertation, University of California, Berkeley

Statements and Declarations

Funding: The first three authors has received research support from the National Natural Science Foundation of China (Grant No. 52078277).

Competing Interests: The authors have no relevant financial or non-financial interests to disclose.

Author Contributions: All authors contributed to the study conception and design. The modeling and analysis were performed by Lei Sun, Xiaodong Ji and Yuncheng Zhuang. The test and data collection were performed by Koichi Kajiwara, Jae-Do Kang and Takuya Nagae. The first draft of the manuscript was written by Lei Sun and Xiaodong Ji. All authors commented on previous versions of the manuscript. All authors read and approved the final manuscript.

Data Availability: The datasets generated during and/or analyzed during the current study are available from the corresponding author on reasonable request.